

# DFT-Spread Spectrally Overlapped Hybrid Orthogonal OFDM-Digital Filter Multiple Access IMDD PONs

Sankoh, Abdulai; Jin, Wei; Zhong, Zhuqiang; He, Jiaxiang; Hong, Yanhua; Giddings, Roger; Tang, Jianming

**Sensors**

Accepted/In press: 30/08/2021

Peer reviewed version

sensors

MDPI

*Article*

# DFT-Spread Spectrally Overlapped Hybrid Orthogonal OFDM-Digital Filter Multiple Access IMDD PONs

**Abdulai Sankoh[1], Wei Jin[1], Zhuqiang Zhong[1,*], Jiaxiang He[1], Yanhua Hong[1], Roger Giddings[1] and Jianming Tang[1]**

1 School of Computer Science and Electronic Engineering, Bangor University, Bangor, LL57 1UT, U.K.
* Correspondence: z.zhong@bangor.ac.uk

**Abstract:** A novel transmission technique namely DFT-spread spectrally overlapped hybrid orthogonal OFDM-Digital filter multiple access (DFMA) PON based on intensity modulation and direct detection (IMDD) is proposed by employing the discrete Fourier transform (DFT)-spread technique in each optical network unit (ONU) and the optical line terminal (OLT). Detailed numerical simulations are undertaken to identify optimum ONU transceiver parameters and explore their maximum achievable upstream transmission performances over the IMDD PON systems. It shows that the DFT-spread technique in the proposed PON is effective in enhancing the upstream transmission performance to its maximum potential, whilst still maintaining all the salient features associated with previously reported PONs. Compared with the previously PON excluding DFT-spread, a significant peak-to-average-power ratio (PAPR) reduction of over 2 dB is achieved, thus leading to a 1 dB reduction in optimum signal clipping ratio (CR). As a direct consequence of the PAPR reduction, the proposed PON has excellent tolerance to reduced digital-to-analog converter/analog-to-digital converter (DAC/ADC) bit resolution and can therefore ensure the utilization of ~~utilize~~ a minimum DAC/ADC resolution of only 6 bits at the forward error correction (FEC) limit ($1\times10^{-3}$). In addition, the proposed PON can improve the upstream power budget by >1.4 dB and increase the aggregate upstream signal transmission rate by up to 10% without degrading nonlinearity tolerances.

**Keywords:** Orthogonal frequency division multiplexing (OFDM); digital filter multiple access (DFMA); DFT-spread OFDM; intensity modulation and direct detection (IMDD); passive optical network (PON)

**Citation:** Sankoh, A.; Jin, W.; Zhong, Z.Q.; Giddings, R.P.; Hong, Y.H.; Tang, J.M. DFT-Spread Spectrally Overlapped Hybrid Orthogonal OFDM-Digital Filter Multiple Access IMDD PONs. *Sensors* **2021**, *21*, x. https://doi.org/10.3390/xxxxx

Academic Editor:

Received: date
Accepted: date
Published: date



## 1. Introduction

To effectively cope with the current avalanche of mobile traffic, driven by the unprecedented increase in users' demands for ultra-wide bandwidth multimedia and cloud services which have become ubiquitous, fronthauls/backhauls of 5G CRANs capable of converging optical and wireless networks are needed, which require significant changes to network access ~~networks~~ in order to support the ambitious system requirements [1,2]. Addressing such technical challenges requires multipronged efforts in different network domains across all layers ~~not only~~ to not only accommodate the explosive expansion in traffic demand~~,~~ but also ~~to~~ efficiently support dynamic bandwidth~~traffic~~ provisioning, improved cost-effectiveness, and power-efficiency [3]. The emergence of software-defined networking (SDNs) with its extended network-control~~led~~ functionalities leverages the abstraction of different physical resources, and enhances the dynamic reconfigurability, flexibility, scalability, and elasticity of the network [4]. To deliver ~~aa~~ SDN-based ~~viable~~ solution capable of satisfying the abovementioned requirements, a non-incremental solution should be implemented to realize the highly desirable cost-effective separately implemented and independently operated legacy optical and wireless access networks in a converged manner. For cost-sensitive application scenarios such as optical access networks, metropolitan area networks (MAN), mobile fronthaul/backhaul networks,

intensity modulation and direct detection-based passive optical networks (IMDD PON) are ~~is~~ considered as a competitive technical solution due to its excellent cost-effectiveness and power efficiency [5].

To overcome the abovementioned technical challenges, a novel PON technique termed hybrid OFDM-DFMA PON utilizing spectrally overlapped digital orthogonal filtering has recently been proposed and extensively investigated [6], where regardless of the ONU count matching filter (MF)-free single fast Fourier transform (FFT) operation and the relevant DSP processes are applied in a pipeline approach. In the proposed PON, transceiver-embedded software reconfigurable digital orthogonal filtering is utilized in each individual ONU, where for upstream transmission two spectrally overlapped digitally filtered orthogonal ONU OFDM sub-band signals occupy the same sub-wavelength spectral region. In the OLT, for ONU sub-band signal demultiplexing and recovery, procedure similar to the ~~earlier~~ previously reported hybrid OFDM-DFMA PONs [7] is adopted~~, where regardless of the ONU count matching filter (MF) free single fast Fourier transform (FFT) operation and the relevant DSP processes are applied in a pipeline approach~~. Numerical result shows that in terms of improving the upstream signal transmission capacity and enhancing the spectral efficiency, the proposed PON outperforms the results ~~the~~ previously ~~earlier~~ reported in [7] by a factor of approximately 2. Moreover, in the context of low OLT-DSP complexity, robustness against practical transceiver impairments, enhanced flexibility, and backward compatibility with existing 4G networks, the proposed PON still maintained all the aforesaid salient unique features ~~which have been known to be~~ associated with the hybrid OFDM-DFMA PONs [6].

It is important to mention that the PONs reported in [6] are OFDM-based. The OFDM's multi-subcarrier modulation scheme is well-known to produce high PAPRs due to the coherent superposition of orthogonal subcarriers in the time domain [8]. Technically speaking, systems with large PAPRs not only require wide dynamic operating ranges for the transceiver-embedded electrical/optical devices, but also produce high quantization noise for a fixed number of quantization bits and may force the involved devices to operate in their non-linear regions, thus introducing nonlinear signal distortions. In addition, ~~the~~ a large PAPR may also cause serious nonlinear noise associated with standard single-mode fiber (SSMF) nonlinearities [9]. Therefore, suppressing ~~the~~ PAPRs in the PONs reported in [6] is of great importance. Several PAPR reduction techniques have been proposed [10-13]. The most widely adopted and simplest approach is to ~~straightforwardly~~ clip ~~the~~ OFDM signals [10,11]. The approach achieves ~~some~~ certain levels of PAPR reduction, however the clipping still ~~can~~ causes significant signal distortions. Another solution is to use multiple signaling and probabilistic techniques such as pilot-assisted partial transmit sequences (PTS) and selected-mapping (SLM) [12,13]. However, due to these approaches requiring redundant information to be transported alongside with ~~the~~ actual data, they have an intrinsic drawback of reducing the useful data rate and increases the computational complexity. In contrast to the abovementioned PAPR reduction techniques, DFT-spread OFDM is the ultimate technical solution, because it is free from parallel redundant information and has low complexity, since only deterministic DFT and IDFT operations are ~~is~~ required in the transceiver [14]. The DFT-spread OFDM technique has already been reported in SSMF IMDD links, including DFT-spread layered/enhanced asymmetrically clipped OFDM systems [15] and probabilistically shaped OFDM enabled IMDD systems [16]. In addition, the DFT-spread technique also processes high compatibility for both long distance [17] and short reach IMDD transmission systems [18] and shows superior performances in PAPR reduction. Recently, we have applied the DFT-spread technique in the hybrid OFDM-DFMA PONs to further improve the system transmission performance flexibility [19]. However, in these~~is~~ PONs, each individual sub-wavelength spectral region just conveys either a single in-phase (I) or quadrature phase (Q) channel upstream double sideband (DSB) OFDM signal only, this gives rise to halving ~~e~~ spectral efficiency compared with the spectrally overlapped hybrid orthogonal OFDM-DFMA PONs [6].

By combining the benefits of the DFT-spread technique and the previously reported PON [6], in this paper, we propose DFT-spread spectrally overlapped hybrid orthogonal OFDM-DFMA IMDD PONs and by numerical simulations, analyze and optimize their performance characteristics. The simulation results show that when the DFT-spread technique is applied, greater than 2dB PAPR reductions are ~~is~~ attained for a digitally filtered OFDM signal carrying QAM modulated data. More importantly, the proposed PON can achieved greater than 1-bit reduction in the minimum required DAC/ADC bit resolution, and larger than 1.4dB upstream power budget improvement. Furthermore, in comparison to the conventional hybrid OFDM-DFMA PON [6], the proposed PON can enhanced the aggregate upstream signal transmission rate by factor of up to 10% in a 25km SSMF IMDD PON transmission system. It is noteworthy that while the proposed PON still maintains all the unique advantages associated with the previously reported PONs [6], in the OLT, without utilizing digital MFs, the single FFT operation followed by summing and subtraction operation of the lower sideband (LSB) and upper sideband (USB) and the corresponding DSP-enabled data recovery processes applied in a pipelined approach cannot only directly demultiplex and demodulate ONU sub-bands signal within the same sub-wavelength spectral region, but also the same OLT-receiver can be used to demodulate legacy OFDM signals.

The above salient features make the proposed PON a feasible solution for future 5G networks in terms of providing DSP-enabled multi-channel aggregation and deaggregation solutions for fronthaul networks [20] to effectively enhance the bandwidth efficiency in comparison with existing common public radio interface (CPRI)-based fronthuals [21]. It should also be pointed out that the proposed PONs are completely different from the multi-band OFDM PON reported in [22], since the PONs proposed here have the following unique features: 1) each sub-wavelength spectral region is shared by two independent orthogonal OFDM sub-band signals [6]; 2) no extra channel spacing is required between adjacent sub-wavelengths or sub-bands; 3) the side lobes of each OFDM sub-band are considerably reduced by the digital filtering process, this can minimize the inter channel interface (ICI) effect between sub-bands at adjacent sub-wavelengths. Furthermore, our results also indicate that for sub-wavelengths that do not suffer the strong channel fading effect, the ICI effects between different orthogonal OFDM sub-bands in these sub-wavelengths are negligible; 4) as a direct result of using the digital filtering process, each OFDM sub-band can adaptively and flexibly adjust its signal modulation parameters such as subcarrier count and channel bandwidth but without affecting the orthogonality between different sub-bands; 5) The digital filtering processing-induced ICI reductions greatly enhance the PON performance and its robustness against the channel frequency offset. In comparison with the up-conversion-based OFDM multi-band PONs, which require multiple tunable electrical local oscillators [20], the spectrally overlapped hybrid orthogonal OFDM-DFMA PONs utilize only digital filters to multiplex multiple OFDM sub-bands without requiring extra electrical/optical components compared to conventional transceivers in both the ONUs and the OLT.

## 2. Principle of DFT-spread Spectrally Overlapped Hybrid Orthogonal OFDM-DFMA PONs

A representative DFT-spread spectrally overlapped hybrid orthogonal OFDM-DFMA IMDD PON architecture is depicted in Fig. 1, in which the more challenging multipoint-to-point upstream operation is considered only. The additional $K$-point DFT and IDFT block at each ONU and OLT combined with a subcarrier mapper and de-mapper module are shown highlighted in yellow. In each ONU, either in-phase (I) or quadrature-phase (Q) M-ary quadrature amplitude modulation-encoded data symbols are grouped into blocks each containing $K$ symbols. The $K$-point DFT operation is applied to spread the symbols into the frequency domain. Localized mapping is then utilized to map the symbols onto an $N$-point ($N$>2($K$+1)) IFFT with $N$-subcarriers. As the first subcarrier is unused, the $K$ signal-carrying subcarriers occupy the first $N$/2-1 subcarriers, as such after

zero padding the signal length is $K \leq N/2 - 1$. To produce a real-valued DFT-spread OFDM signal, an $N$-point IFFT operation is applied after enforcing the Hermitian symmetry. Following the cyclic prefix (CP) addition, each sub-band digitally encoded sample sequence is up-sampled by a factor $M\times$. After that, the digital shaping filters after having fed the up-sampled sequence generated a digitally filtered sub-band signal, which are pass through the DAC and then fed into an optical intensity modulator (IM) to perform electrical-to-optical (E-O) conversion. Similar to the treatment adopted in [7], the utilization of IM as the preferred light source in the numerical simulations is to completely eliminate the signal-signal beating interference (SSBI) effect [23]. It is noteworthy that, for practical implementation of the proposed PONs, different ONUs can use different wavelengths to transmit their OFDM sub-bands, provided that ~~and~~ every two adjacent wavelengths have a minimum wavelength space of ~0.28nm in order to ~~to~~ mitigate the SSBI effects effectively [24].

After transmitting through an SSMF, in the OLT the corresponding receiver DSP functions are as follows; signal detection by a photo-detector (PD), signal digitization by an ADC, serial-to-parallel conversion, symbol timing alignment, CP removal, single $L$-point FFT operation with $L$ satisfying $L=MN$ for generating complex-valued frequency domain subcarriers utilizing the received real-valued time domain symbols, lower sideband (LSB) and upper sideband (USB) subcarriers identification, independent channel estimation and channel equalization of LSB and USB subcarriers based on the pilot subcarriers, and sideband processing to demultiplex the spectrally overlapped spectrum spread OFDM subcarriers. After the above DSP process, the resulting output sub-band subcarriers data are passed through the subcarrier de-mapper. The output of the de-mapper is then subjected to the $K$-point IDFT and symbol demodulation to obtain data information corresponding to the transmitted I-phase and Q-phase ONUs sub-band input data.

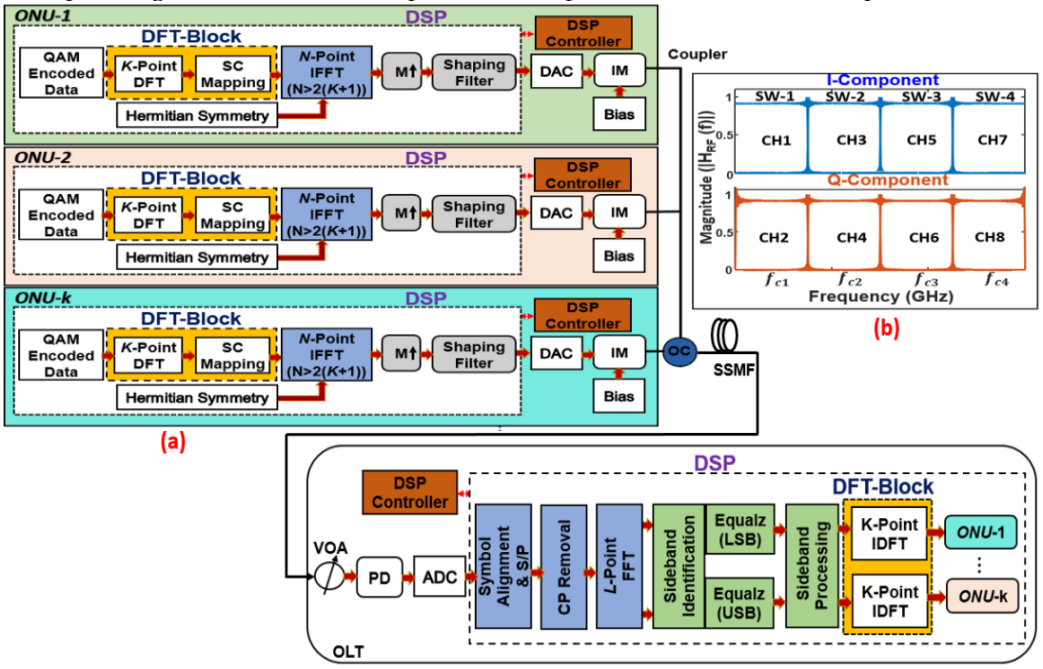


**Figure 1.** (a) DFT-spread hybrid orthogonal OFDM-DFMA PON (b) Example of digital filter allocation and digital filter frequency response, all digital filters are produced using a Hilbert-pair approach. SC: subcarrier, DFT: discrete Fourier transform, M↑: up-sampling factor, DAC/ADC: digital-to-analogue/analogue-to-digital converter. IM: intensity modulator. OC: optical coupler, SSMF: standard single-mode fiber, VOA: variable optical attenuator, PD: photodetector. S/P: serial-to-parallel conversion, Equalz: equalization, ONU: optical network unit, OLT: optical line terminal, DSP: digital signal processing, SW: sub-wavelength, CH: channel.

## 3. Upstream Optimum ONU Operating Conditions

In performing the numerical simulations over a 25 km SSMF, an IMDD PON theoretical model developed and verified in [6] is adopted, where the procedure detailed in [25] is used to simulate the ~~O~~optical OFDM signal generation, nonlinear transmission, and direct detection.

*3.1. Simulation Models and Key Parameters*

In this paper, 2-ONUs are considered, each producing an optical sub-band signal sharing the same sub-wavelength with the other ONU. To conduct the simulations, MATLAB tools are ~~is~~ used for signal generation and detection, while the VPI TransmissionMaker is used for optical fiber transmission. To implement the shaping filter in each individual ONU, the Hilbert-pair approach [26,27] is adopted to construct the digital orthogonal filters consisting of two spectrally overlapped I-phase and Q-phase orthogonal ONU sub-band signals. To support 2 independent ONUs, the up-sampling factor is set at M=2 [26]. Since the DAC/ADC operates at 12.5 GS/s and the 2-ONUs occupy the same spectral region, the signal bandwidth for each ONU is equal to the Nyquist frequency, $fs/M$, and the central frequency of the orthogonal digital filter-pair is $fs/2M$, where $fs$ is the DAC/ADC sampling speed. For the ~~case~~ M=2 case, Fig. 2(a) and (b) illustrate the spectral locations of digitally filtered sub-band signals (I-phase and Q-phase) and their spectra. To generate a real value OFDM signal necessary for intensity modulation, a 32-point IFFT size is considered, in which 15 subcarriers in the positive frequency bins convey real data, one subcarrier ~~–~~contains no power, and the remaining 16 subcarriers in the negative frequency bins are the complex conjugate of data bearing subcarriers. To reduce the power leakage caused by crosstalk between spectrally overlapped digital orthogonal sub-bands and maximize the upstream signal transmission capacity, 14 data-bearing subcarriers out of 15 are employed to deliver the ~~allow for~~ acceptable upstream performance for each sub-band. The DFT block size $K$ is thus set to be 14. It is however expected that all of the 15 subcarriers can be supported if channel interference mitigation techniques are applied [28,29]. In this demonstration all the subcarriers are encoded with a 64-QAM signal modulation format, however any modulation formats are applicable.

**Table 1**: SYSTEM PARAMETERS

| Parameter | Value | Parameter | Value |
|---|---|---|---|
| IFFT/ FFT Size | 32/64 | Clipping Ratio- Including /Excluding DFT-spread | 11 dB / 12 dB |
| Number of Used Data Subcarriers Per ONU | 14 | Digital Filter Length/ Excess of the Bandwidth | 64/0 |
| Modulation Format | 64-QAM | PIN Detector Quantum Efficiency | 0.8 A/W |
| Cyclic Prefix | 25% | PIN Detector Sensitivity | -19 dBm |
| Channel Bitrate | 13.12 Gb/s | PIN Detector Bandwidth | Ideal |
| Optical Launch Power | 0 dBm | Fiber Dispersion | 17 ps/nm/km |
| DAC/ADC Sample Rate | 12.5 GS/s | Fiber Dispersion Slope | 0.08 ps/nm$^2$/km |
| Number of Bits | 7-bits | Fiber Loss | 0.2 dB/km |
| Up-sampling Factor | M=2 | Fiber Kerr Coefficient | $2.6\times10^{-20}$ m$^2$/W |
| FEC Limit [1] | $1\times10^{-3}$ | Transmission Distance | 25 km |

[1] Corresponding to 10 Gb/s non-return-to-zero data at a BER of $1.0\times10^{-9}$

Detailed explorations of the impact of quantization and clipping noise on the upstream transmission performance of the digitally filtered spectrum spread OFDM signals are undertaken in Section 3.3, in which an optimum 7-bits resolution and optimum clipping ratios of 11 dB and 12 dB are identified for the cases of including and excluding the DFT-spread respectively. These identified optimum parameters are adopted throughout

this paper. Unless otherwise stated, all other system parameters are summarized in Table 1.

In the OLT, an ideal positive-intrinsic-negative (PIN) photodetector for direct detection of the optical signal is employed, with a receiver sensitivity of -19 dBm and quantum efficiency of 0.8 A/W. Both shot noise and thermal noise are considered, which are simulated using procedures similar to those presented in [30]. In addition, the OLT-based receiver consists of a variable optical attenuator (VOA) to adjust the received optical power (ROP) level and the ADC incorporates an ideal antialiasing electrical filter with a 6.25 GHz bandwidth to remove out-of-band receiver noise before signal sampling.

By taken into account the transceiver parameters listed in Table 1 and the adopted signal modulation formats, the upstream signal transmission rate per ONU is ~13.12 Gb/s, and the aggregate upstream PON transmission rate is ~26.25 Gb/s. It is noteworthy that due to the high attenuation of ~~the~~ the filter near the DC component, only 14 subcarriers (2 to 15) are activated ~~enabled~~ in each ONU as the first subcarrier contains no power.

### *3.2. PAPR Performance of DFT-spread Hybrid Orthogonal OFDM-DFMA PON*

Having chosen the simulation parameters, identified the optimum conditions, and understood the operating principle of the proposed DFT-spread spectrally overlapped hybrid orthogonal OFDM-DFMA IMDD PON, in this section, we numerically explore the PAPR reduction efficiency of the proposed PON consisting of 2 ONUs. Fig. 2 (a) and (b) show the spectral locations of two digitally filtered sub-band signals (I-phase and Q-phase) and their spectra. In addition, the comparative complementary cumulative distribution function (CCDF) of the PAPR including and excluding DFT-spread are presented in Fig. 2 (c) and (d) for various digital filter lengths ranging from 16 to 256, and signal modulation format varying from 16-QAM to 256-QAM ~~are presented in Fig. 2 (c) and (d)~~. For the sake of simplicity, only the ONU-2 referred to as channel-2 CCDF curve is plotted for both cases as ONU-1 referred here as channel-1 curves are similar to channel-2.

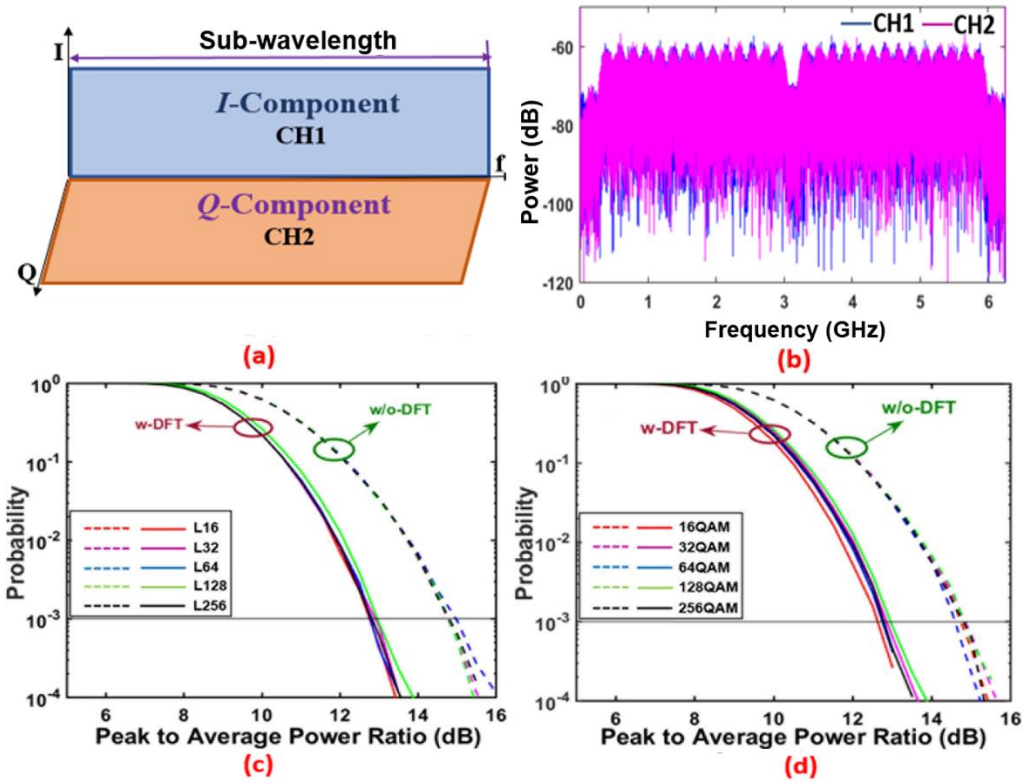


**Figure 2.** (a) Spectral location of orthogonally digitally filtered sub-band signals (I-phase and Q-phase) and (b) their spectra. CCDFs of PAPR for (c) varying digital filter lengths and fixed 64-

QAM modulation format and (d) varying modulation formats and fixed digital filter length of L=64.

It can be seen from Fig. 2 that compared to the case without DFT-spread, the case with DFT-spread can reduce the PAPR ratio by ~~as large as or greater than ≥~~2 dB at the CCDF value of $1\times10^{-3}$ when the optimum clipping ratio of 11 dB is adopted. The results are similar to our previous work and observed in WDM-PONs ~~as well~~ [19,31]. It is also very interesting to note in Fig. 2(c) and Fig. 2(d) that the proposed PON upstream transmissions have very similar PAPR performances for varying both digital filter lengths up to 256 and signal modulation formats to 256-QAM. This indicates that the DFT-spread induced PAPR-reductions are independent of the digital filter length and signal modulation. Moreover, the obtained results also suggest that under the same transmit power constraint, the DFT-spread case with a low PAPR can achieve a higher optical signal-to-noise ratio (OSNR), ~~. This being~~ this is one of the factors leading to the increased upstream channel rate presented in section 4.2. This statement is confirmed in Fig. 6. Nevertheless, it is worth noting that the performance of the PONs reported in [6] are largely limited by digital filter-induced signal distortions. As such, in this paper ~~and as listed in Table 1~~, to highlight the unique features of the DFT-spread technique, a digital filter length of 64, as listed in Table 1, is utilized to minimize the digital filter impairments.

From the above discussion, it is easy to understand that the proposed PON induced PAPR reduction gives rise to an excellent improvement in system performance robustness to ~~the~~ quantization noise induced by ~~the~~ limited DACs/ADCs bit resolutions. In addition, it also relaxes the constraints on linear dynamic operating ranges of the transceiver-embedded optical/electrical devices, reduces the optical nonlinearity impairments, and ~~so~~ allows the reduction in the DSP complexity and overall cost of the transceivers.

### *3.3. Optimum Clipping Ratio and DAC/ADC Resolution Bits*

In order to numerically explore the feasibility of utilizing the proposed technique to improve the upstream transmission performance of the PON, in this section numerical simulations are first undertaken to identify the optimum operating condition for achieving the best possible performance. Fig. 3 presents the simulated bit error rate (BER) contours as a function of quantization bit~~s~~ and clipping ratio (CR) for an optical back-to-back (B2B) configuration. In obtaining these figures, the ROP at the OLT is fixed at -7 dBm. Since the 2-ONUs are independent and have the same signal characteristics, without loss of generality only channel-2 is plotted in Fig.3.~~.~~

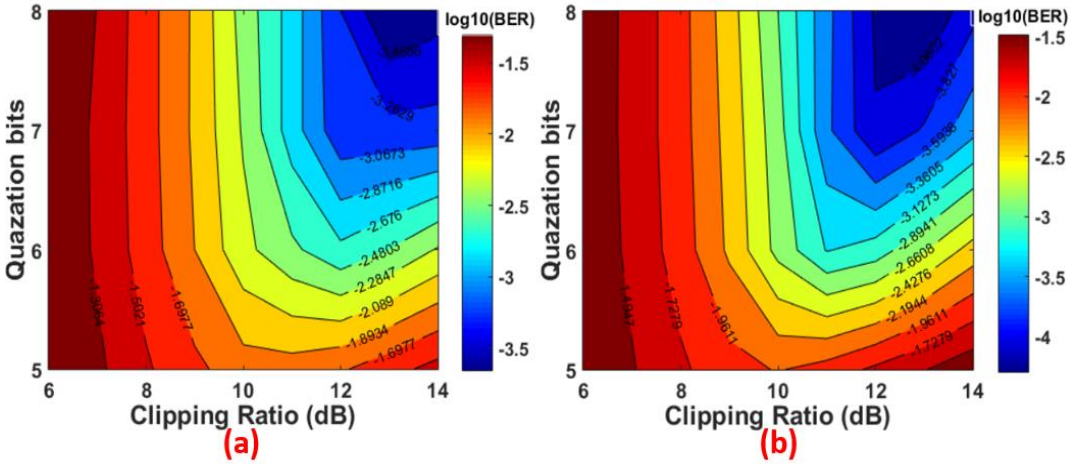


**Figure 3**. BER contour versus quantization bit resolution and clipping ratio for (a) excluding the DFT-spread (b) including the DFT-spread.

It can be seen in Fig. 3 that when ~~the~~ a CR is low, the overall channel BER performance is high because the signal waveform is significantly clipped. In these figures, for a fixed

bit resolution within ~~the~~ a dynamic range from 7 to 8 bits, for maintain~~ed~~ BERs below the FEC limit ($1\times10^{-3}$), the ~~the~~ CR should be ≥11 dB for the DFT-spread case. On the other hand, for the case without DFT-spread over the same dynamic region, the CR should be ≥12dB, which shows an increase in CR by 1dB. From the same figures it can also be observed that the case excluding DFT-spread has a CR dynamic range of 12dB≤CR≤14dB, while the case including DFT-spread achieves a CR dynamic range of 11dB≤CR≤14dB. Outside these regions, ~~values,~~ the BER increases with increasing CR because of the rise in the quantization noise effect and decreasing the CR causes the creation of in-band/out-band noise due to clipping distortions. The result ~~thus~~ indicates that the proposed PON can reduce the DAC/ADC bit resolution by 1 bit, i.e., form 7 bits to 6 bits, and reduce the CR by ≥1 dB for ~~to~~ achieving BERs at the FEC limit. This behavior clearly demonstrates that the proposed PON with the application of the DFT-spread technique allows the transceiver to adopt low CRs, without greatly compromising the BER performances. Based on the above analysis, ~~these~~ the identified optimum CR values and DAC/ADC resolution of 7-bits are chosen to enable the ONUs to operate at their optimum conditions. The obtained results for the optimum parameters are presented in Table 1.

## 4. Upstream DFT-spread Hybrid Orthogonal OFDM-DFAM PON Performance

Utilizing the optimum ONU operating conditions identified in Section 3 and the transceiver parameters listed in Table 1, in this section the investigations of ~~the~~ upstream transmission performance of a spectrally overlapped hybrid orthogonal OFDM-DFMA PON incorporating the DFT- spread technique are undertaken in terms of upstream performance tolerance to limited DAC/ADC quantization bits, BER performance, maximum aggregate upstream signal transmission rate, and impact of digital filter impairments. To highlight the advantages associated with the proposed technique, the upstream transmission performances of the hybrid OFDM-DFMA PON utilizing spectrally overlapped digital orthogonal filtering are also computed, which are treated as benchmarks.

### *4.1. Performance Tolerance to Limited DAC/ADC Quantization Bits*

In this subsection, simulations are carried out to demonstrate the performance tolerance of the proposed technique to limited DAC/ADC quantization bits and to determine the minimum number of required DAC/ADC quantization bits to achieve BERs at or below the FEC limit. The DAC/ADC quantization bits vary from 4 to 8 and the ROP is fixed at -7dBm. The results are presented in Fig. 4 for the 25 km SSMF IMDD PON.

Fig. 4 reveals that, while adopting the optimum CRs of 11 dB or 12 dB as determined in section in 3.3, the case including DFT-spread can reach BERs at the FEC limit when the DAC/ADC resolution is as low as 6 bits. On the other hand, for the case excluding DFT-spread, the minimum number of the required quantization bits for achieving the similar performance extends from 6 bits DAC/ADC resolution to 7 bits. The numerical result confirms that the application of DFT-spread in the proposed PON can improve the upstream performance tolerance against ~~to~~ quantization noise induced by the limited quantization bits. Most importantly, from a practical PON operation point of view, such improvement is highly desirable for PON designs as lower DAC/ADC hardware achieves both lower cost and low power consumption.

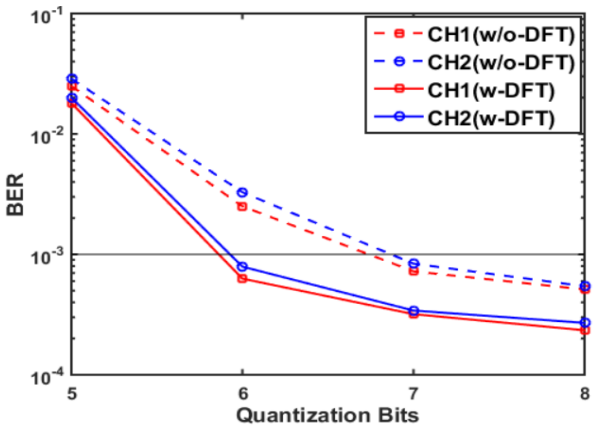


**Figure 4**. BER versus quantization bits over 25 km SMMF IMDD PON.

From the above discussion, it is easy to understand that the proposed DFT-spread spectrally overlapped hybrid orthogonal OFDM-DFAM PON confirms the practicability of utilizing the DFT-spread technique in the PONs reported in [6], and that the proposed PON has the ability to reduce the minimum required DAC/ADC bit resolution and so consequently minimize the transceiver DSP complexity, thus making the proposed PON a promising solution for implementation in a cost-sensitive future 5G and beyond networks.

### 4.2. Upstream Transmission Performance

Fig. 5 is the overall channel BER as a function of the received optical power where the total optical launch power into the SSMF transmission system is fixed at 0 dBm. In computing Fig. 5, a resolution of 7 bits as shown in Fig. 4 are used for the ADC/DAC. All other parameters are specified in Table 1.

It can be seen in Fig. 5 that for the case of including/excluding DFT-spread, the calculated channel 1 (CH1) and channel 2 (CH2) BER performances are identical across the entire received optical power range and these two channels also have very similar signal bit rates. Most importantly, for the same signal bit rates, the case with DFT-spread can achieve an upstream power budget improvement of greater than 1.4dB compared to the case without DFT-spread. Such performance improvement is mainly because of the DFT-spread-induced PAPR reduction, resulting in a considerable decrease in quantization noise, thus giving rise to an increase in the effective OSNRs.

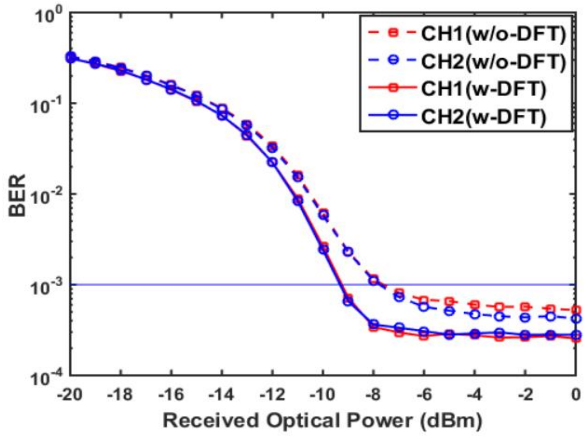


**Figure 5.** BER versus received optical power after 25 km SSMF IMDD PON transmission system when 7 bits resolution is considered.

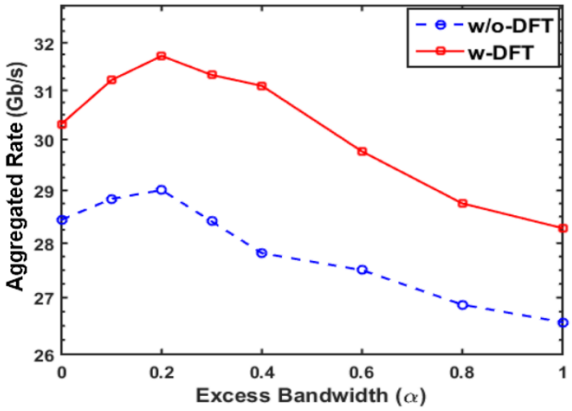


**Figure 6.** Aggregated rate versus excess bandwidth after 25 km SSMF IMDD PON transmission system when 7 bits resolution is considered.

### *4.3. Impacts of Digital Filter Parameters on Maximum Aggregated Upstream Transmission Rates*

For the proposed PON simultaneously supporting two ONUs, the aggregated upstream signal transmission capacities versus excess of bandwidth parameter, $\alpha$, are shown in Fig. 6. In obtaining Fig. 6, the digital filter length ~~is~~ listed in Table 1 is adopted. In addition, adaptive bit-loading is applied to all subcarriers involved in each ONU for all the cases of including and excluding DFT-spreading. To implement adaptive bit-loading, the highest possible signal modulation formats within the range from DBPSK to 256-QAM is adaptively selected according to the channel spectral characteristics to ensure that ~~, which, considering that~~ the BER across all subcarriers for each sub-band can reach the FEC limit of $1\times10^{-3}$. For each ONU sub-band, the achievable signal bit rate is $R_b = f_s \sum_{k=1}^{N_s} n_{kb}/2(N_s+1)\left(1+C_p\right).M$, where $n_{kb}$ is the number of binary bits conveyed by the $kth$ subcarrier within one OFDM symbol period, $N_s$ denotes the number of data-bearing subcarriers, and $C_p$ indicates the overhead parameter associated with the cyclic prefix and training sequences. The excess of bandwidth $\alpha$, is set to vary in the range $0\leq\alpha\leq1$. The ROPs are fixed at -6 dBm for both cases.

It can be seen in Fig. 6 that for both considered cases, the aggregate upstream signal transmission rate peaks at an $\alpha$ factor value of 0.2 and then reduces steadily as $\alpha$ increases above 0.2. Most importantly, for the case including DFT-spread, the maximum aggregate upstream signal transmission rate increases by up to 10% for $\alpha$=0.2, compared to the case without DFT-spread. This performance enhancement is due to the overall improvement in SNRs across the subcarriers, thus allowing higher modulation formats to be used. To understand the physical mechanisms causing an optimum $\alpha$ value of 0.2, the impact of $\alpha$ on the digital filter responses should be observed. For low $\alpha$ values <0.2, the finite filter length-induced filter magnitude response ripples can impact on performance. For the case of $\alpha$=0, the I-phase filter (channel 1) has a perfectly flat response as the up-sampling factor M=2 is considered [26], while the Q-phase filter (channel 2), has significant frequency response ripples as shown in Fig. 7(a) and (b) respectively [26]. The length of the filter mainly impacting the sharpness of the filter edge for the case of the Q-phase filter. On the other hand, as shown in Fig. 7(c) and (d), as $\alpha$ starts to increase there is a boost in the magnitude response of the I-phase filter and an attenuation in the magnitude response of the Q-phase filter, in addition the increasing distortion of the filter responses causes strong unwanted cross-channel induced interference due to loss of orthogonality. Note, that this filter response distortion occurs due to aliasing effects as the employed sub-wavelength occupies the whole Nyquist band. The increasing $\alpha$ value also reduces the unwanted frequency response ripples in the Q-phase filter. These effects combine to give an overall

increase in subcarrier SNR as $\alpha$ increases from 0 to 0.2, beyond which there is an overall reduction in subcarrier SNR.

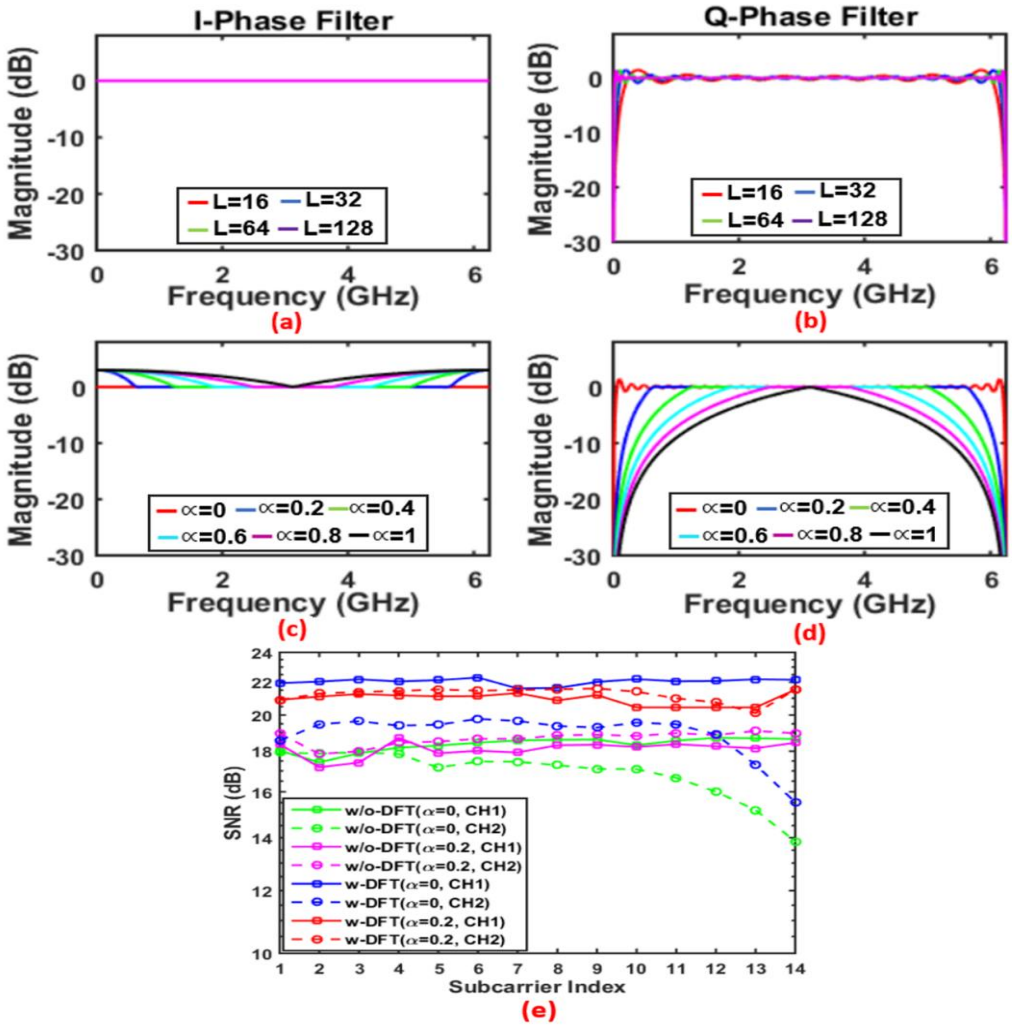


**Figure 7**. Magnitude response for excess of bandwidth of $\alpha$=0 for (a) I-phase filter with digital filter length L=16, 32, 64 and 128 (b) Q-phase filter with digital filter length L=16, 32, 64 and 128. Magnitude response for filter length, L=64 (c) I-phase filter with excess of bandwidth ($\alpha$) ranging from 0 to 1 (d) Q-phase filter with excess of bandwidth ($\alpha$) ranging from 0 to 1. (e) Comparison of SNR distribution across all the subcarriers using excess of bandwidth of $\alpha$=0 and optimum value of $\alpha$=0.2 for both I-phase (CH1), and Q-phase (CH2).

To observe the effect of $\alpha$ on subcarrier SNRs, with the simultaneous presence of both channels, the SNR performances for all subcarriers for the 25 km SSMF transmission are plotted in Fig. 7(e) utilizing the optimum $\alpha$ parameter value of 0.2 and zero excess of bandwidth ($\alpha$=0) for performance comparisons. In obtaining this figure, the ROP is fixed at -6 dBm. Fig. 7(e) shows that the SNRs are similar for CH1 when $\alpha$=0 and $\alpha$=0.2, however, there is an obvious improved SNR for subcarrier index 12-14 of CH2 when $\alpha$=0.2. It also shows that the SNR curve for CH1 is almost constant with respect to the subcarrier index for the optimum $\alpha$ value. In comparison with the Q-phase channel for both cases, the high SNR observed for the I-phase channel is mainly because of the boost in the magnitude response, as shown in Fig. 7(c). The obtained results indicate that there is an optimum $\alpha$ factor value which minimizes digital filter impairments and subsequently maximizes the upstream transmission rate of both channels.

## 5. Conclusions

The novel DFT-spread spectrally overlapped hybrid orthogonal OFDM-DFMA PON is proposed and numerically simulated for a 25 km IMDD SSMF transmission system. To the best of our knowledge, it is the first work ~~example~~ of applying the DFT-spread technique in the hybrid OFDM-DFMA PONs utilizing spectrally overlapped digital orthogonal filtering, in order to simultaneously reduce PAPRs, optimize CRs, and reduce the minimum required DAC/ADC quantization bits whilst maintaining the upstream transmission performances and increasing the transceiver complexity. The simulation results have shown that, compared to the previously reported PONs, the proposed PON can reduce the PAPR by greater than 2 dB and the optimum CR is reduced by 1dB. Such a PAPR reduction is independent of the adopted digital filter characteristic~~s~~, signal modulation format~~s~~ and ONU sub-band signal spectral location. As a direct result of the PAPR reduction, the proposed PON can reduce the minimum required DAC/ADC resolution bits by more than 1-bit whilst achieving BERs below the FEC limit. In addition, the proposed PON can improve the upstream power budget by greater than 1.4 dB and increase the aggregate upstream signal transmission rate by up to 10%.

It is well known that the ~~For achieving high bandwidth transmissions, high speeds of~~ –DACs and ADCs play an important role in limiting the ~~are required~~maximum achievable signal transmission capacity for DSP-based signal transmission techniques. However, high-speed DACs and ADCs can be very expensive. To achieve a specific signal transmission capacity, the proposed technique has the potential of allowing low-speed DACs/ADCs to be utilized to produce/receive targeted baseband signals, which can then be up-converted to the targeted sub-bands by low-cost electrical components. This could significantly reduce the overall ONU transceiver cost. In addition, ~~in the proposed technique. However, in practical implementations, to greatly reduce the overall network expenditures, the ONUs occupying low radio frequency spectral regions may use low-speed DACs/ADCs to produce/receive their targeted sub-bands. The low-speed DACs/ADCs may also be applicable in the ONUs occupying high radio frequency spectral regions with the help of extra low-cost electrical components such as up-converters. Furthermore,~~ the proposed technique-induced ~~with great capability of reducing~~ PAPR reductions ~~s~~also considerably ~~will~~ relax the requirements of using expensive electrical/optical devices with large linear operation regions and high-resolution DACs/ADCs. As a direct result, ~~,~~ ~~thus~~ the proposed technique may offer ~~presenting a~~ a valuable solution capable of ~~to~~ reducing ~~e~~ the overall network installation cost for implementation in cost-sensitive application scenarios. ~~expenditures.~~

The experimental demonstrations of point-to-point and multipoint-to-point spectrally overlapped hybrid orthogonal OFDM-DFMA PON transmissions with/without DFT-spreading are currently being undertaken in our research laboratory and corresponding results will be reported elsewhere in due course.

**Author Contributions:** Conceptualization, Wei Jin and Jianming Tang; Data curation, Abdulai Sankoh and Jiaxiang He; Formal analysis, Abdulai Sankoh; Funding acquisition, Jianming Tang; Methodology, Wei Jin; Project administration, Jianming Tang; Software, Abdulai Sankoh; Supervision, Zhuqiang Zhong, Yanhua Hong, Roger Giddings and Jianming Tang; Validation, Abdulai Sankoh, Zhuqiang Zhong, Roger Giddings and Jianming Tang; Visualization, Abdulai Sankoh and Jiaxiang He; Writing – original draft, Abdulai Sankoh; Writing – review & editing, Wei Jin, Zhuqiang Zhong, Yanhua Hong, Roger Giddings and Jianming Tang.

All authors will be informed about each step of manuscript processing including submission, revision, revision reminder, etc. via emails from our system or assigned Assistant Editor.

**Funding:** This research was funded in part by the DESTINI project funded by the ERDF under the SMARTExpertise scheme, and in part by the DSP Centre funded by the ERDF through the Welsh Government.

**Institutional Review Board Statement:** Not applicable

**Informed Consent Statement:** Not applicable

**Data Availability Statement:** Not applicable

**Acknowledgments:** This work was supported in part by the DESTINI project funded by the ERDF under the SMARTExpertise scheme, and in part by the DSP Centre funded by the ERDF through the Welsh Government.

**Conflicts of Interest:** The authors declare no conflict of interest.

## References

1. Dogra, A.; Jha, R.K.; Jain, S. A survey on beyond 5G network with the advent of 6G: architecture and emerging technologies. *IEEE Access* **2021**, 9, 67512-67547.
2. Ruffini, M. Multidimensional convergence in future 5G networks. *J. Light. Technol.* **2017**, 35, 535-549.
3. Gavrilovska, L.; Rakovic, V.; Ichkov, A.; Todorovski, D.; Marinova, S. Flexible C-RAN: radio technology for 5G. 1*3th Int. Conf. on Advanced Technol., Systems and Services in Telecom. (TELSIKS*), **2017**, 255-264.
4. Ramantas, K.; Antonopoulos, A.; Kartsakli, E.; Mekikis, P.; Vardakas J.; Verikoukis, C. A C-RAN based 5G platform with a fully virtualized, SDN controlled optical/wireless fronthaul. *20th Int. Conf. on Transp. Opt. Netw. (ICTON)* **2018**, 1-4.
5. Fu, M.; Zhuge, Q.; Liu, Q.; Fan, Y.; Zhang, K.; Hu, W. Advanced optical transmission technologies for 5G fronthaul. *24th Opto-Electronics and Commun. Conf. (OECC) and Int. Conf. on Photo. in Switch. and Comp. (PSC)* **2019**, 1-3.
6. Sankoh, A.; Jin, W.; Zhong, Z.Q.; He, J.; Hong, Y.; Giddings, R.P.; Pierce, I.; O'Sullivan, M.; Lee, J.; Durrant, T.; Tang, J.M. Hybrid OFDM-Digital filter multiple access PONs utilizing spectrally overlapped digital orthogonal filtering. *IEEE Photo. J.* **2020**, 12, 1-11.
7. Dong, Y.X.; Giddings, R.P.; Tang J.M. Hybrid OFDM-digital filter multiple access PONs. *J. Light. Technol.* **2018**, 36, 5640–5649.
8. Cvijetic, N. OFDM for next generation optical access networks. *Opt. Fiber Commun. Conf. and Exposition and the Nat. Fiber Opt. Eng. Conf.* **2011**, 1-30.
9. Silva, J.A.L.; Cartaxo, A.V.T.; Segatto, M.E.V. A PAPR reduction technique based on a constant envelope OFDM approach for fiber nonlinearity mitigation in optical direct-detection systems. *J. Opt. Commun. Netw.* **2012**, 4, 296-303.
10. Vappangi, S.; Mani, V.V. A low PAPR DST-based optical OFDM (OOFDM) for visible light Communication. *21st Int. Symposium on Wireless Personal Multimedia Commun. (WPMC)* **2018**, 200-205.
11. Xu, W.; Wu, M.; Zhang, H.; You, X.; Zhao, C. ACO-OFDM-specified recoverable upper clipping with efficient detection for optical wireless communications. *IEEE Photo. J.* **2014**, 6, 1-17.
12. Popoola, W.O.; Ghassemlooy, Z.; Stewart, B.G. Pilot-Assisted PAPR reduction technique for optical OFDM communication systems. *J. Light. Technol.* **2014**, 32, 1374-1382.
13. Nadal, L.; Moreolo, M.S.; Fabrega, J.M.; Junyent, G. Comparison of peak power reduction techniques in optical OFDM systems based on FFT and FHT. *13th Int. Conf. on Transparent Opt. Netw.* **2011**, 1-4.
14. Shieh, W.; Tang, Y.; Krongold, B.S. DFT-spread OFDM for optical communications. *9th Int. Conf. on Opt. Internet (COIN)* **2010**, 1-3.
15. Bai, R.; Wang, Z.; Jiang, R.; Cheng, J. Interleaved DFT-spread layered/enhanced ACO-OFDM for intensity-modulated direct-detection systems. *J. Light. Technol.* **2018**, 36, 4713-4722.
16. Ma, J.; Chen, M.; Wu, K.; He, J. Performance enhancement of probabilistically shaped OFDM enabled by precoding technique in an IM-DD system. *J. Light. Technol.* **2019**, 37, 6063-6071.
17. Wang, Y.; Yu, J.; Chi, N. Demonstration of 4×128-Gb/s DFT-S OFDM signal transmission over 320-km SMF with IM/DD. *IEEE Photo. J.* **2016**, 8, 1-9.
18. Chen, M.; Xiao, X.; Huang, Z.R.; Yu, J.; Li, F.; Chen, Q.; Chen, L. Experimental demonstration of an IFFT/FFT size efficient DFT-spread OFDM for short reach optical transmission systems. *J. Light. Technol.* **2016**, 34, 2100-2105.
19. Dong, Y.X.; Jin, W.; Giddings, R.P.; O'Sullivan, M.; Tipper, A.; Durrant, T.; Tang, J.M. Hybrid DFT-spread OFDM-digital filter multiple access PONs for converged 5G networks. *IEEE J. of Opt. Comm. and Netw.* **2019**, 11, 347-353.
20. Wake, D.; Nkansah A.; Gomes, N.J. Radio over fiber link design for next generation wireless systems. *J. of Light. Technol.* **2010**, 28, 2456-2464.
21. Liu, X.; Zeng, H.; Chand N.; Effenberger, F. Efficient mobile fronthaul via DSP-based channel aggregation. *J. of Light. Technol.* **2016**, 34, 1556-1564.
22. Chandrasekhar, S.; Liu, X. OFDM based super channel transmission technology. *J. Light. Technol.* **2012**, 30, 3816-3823.
23. Jung, S.M.; Mun, K.H.; Jung, S.Y.; Han, S.K. Optical-beat-induced multi-user-interference reduction in single wavelength OFDMA PON upstream multiple access systems with self-homodyne coherent detection. *J. Light. Technol.* **2016**, 34, 2804-2811.
24. Jin, W.; Zhong, Z.Q.; He, J.X.; Sankoh, A.; Giddings, R.P.; Hong, Y.H.; Pierce, I.; O'Sullivan, M.; Laperle, C.; Lee, J.; Mariani, G.; Durrant, T.; Tang, J.M. Experimental demonstrations of hybrid OFDM-digital filter multiple access PONs. *IEEE Photon. Technol. Lett.* **2020**, 32, 751–754.

25. Tang J.M.; Shore, K.A. 30-gb/s signal transmission over 40-km directly modulated DFB-laser-based single-mode-fiber links without optical amplification and dispersion compensation. *J. of Light. Technol.* **2006**, 24, 2318-2327.
26. Bolea, M.; Giddings, R.P.; Tang, J.M. Digital orthogonal filter- enabled optical OFDM channel multiplexing for software-reconfigurable elastic PONs. *J. Light. Technol.* **2014**, 32, 1200–1206.
27. Bolea, M.; Giddings, R.P.; Bouich, M.; Aupetit-Berthelemot, C.; Tang, J.M. Digital filter multiple access PONs with DSP-enabled software reconfigurability. *J. Opt. Commun. Netw.* **2015**, 7, 215–222.
28. Dong, Y.X.; Al-Rawachy, E.; Giddings, R.P.; Jin, W.; Nesset, D.; Tang, J.M. Multiple channel interference cancellation of digital filter multiple access PONs. *J. Light. Technol.* **2017**, 35, 34–44.
29. Al-Rawachy, E.; Giddings, R.P.; Tang, J.M. Experimental demonstration of cross-channel interference cancellation for digital filter multiple access PONs. *Opt. Express* **2016**, 25, Th3C.5.
30. Agrawal, G.P. *Fibre-optic communication systems*, 3rd ed. Rochester, NY, USA, 2002, pp. 133–176.
31. Zeng Y.; Dong Z.; Chen Y.; Wu X.; He H.; You J.; Xiao Q. A Novel CAP-WDM-PON employing multi-band DFT-spread DMT signals based on optical Hilbert-transformed SSB modulation. *IEEE Access* **2019**, 7, 29397-29404.